machines

MDPI

Article

The Formation of a Low-Carbon Steel/Ni-Cr-W Alloy Bimetallic Material via Liquid–Solid Compound Casting with a Laser Assisted Solid Surface

Serhii Salii [1], Leonid Golovko [1], Oleksii Kaglyak [1], Oleksandr Kapustynskyi [2] and Nikolaj Višniakov [3,*]

[1] Department of Laser Systems and Advanced Technologies, National Technical University of Ukraine "Igor Sikorsky Kyiv Polytechnic Institute", 37, Prospect Beresteiskyi, 03056 Kyiv, Ukraine; saliysergiys@gmail.com (S.S.); leongolovko@gmail.com (L.G.); kaglyak.olexa@gmail.com (O.K.)
[2] Department of Mechanics and Material Engineering, Vilnius Gediminas Technical University, Plytines g. 25, LT-10105 Vilnius, Lithuania; o.kapustynskyi@vilniustech.lt
[3] Institute of Mechanical Science, Vilnius Gediminas Technical University, Plytines g. 25, LT-10105 Vilnius, Lithuania
* Correspondence: nikolaj.visniakov@vilniustech.lt

Abstract: The aim of this study was to develop a new manufacturing process for bimetallic materials by combining laser treatment with traditional casting methods. This process involves laser-treating nickel alloy-grade UNS 6230 plates to create a regular macro-relief on their surface. These treated plates are then placed in a sand mold, and molten non-alloy steel (S235JRG2) is poured into the mold to create bimetallic layered castings. The experimental procedure focuses on optimizing the melt-to-solid phase ratios and pouring temperatures to achieve a uniform microstructure and strong mechanical properties in the bimetals. The produced bimetallic castings are suitable for applications in the oil refining and chemical industries and heavy machinery sector. The quantitative results indicate that the optimized process parameters lead to a high-quality transition zone with minimal defects, characterized by the diffusion of alloying elements from the nickel alloy to the steel. The microstructure, chemical, and phase compositions were evaluated using XRD and SEM with EDS, confirming the formation of a robust metallurgical bond. Key findings include a significant improvement in the hardness and strength of the transition layer, with the optimal pouring temperature being 1600 °C. The resulting bimetallic materials demonstrate an improved performance in demanding industrial environments.

Keywords: laser treatment; bimetallic joint; bimetallic materials; multi-layered materials

check for updates

Citation: Salii, S.; Golovko, L.; Kaglyak, O.; Kapustynskyi, O.; Višniakov, N. The Formation of a Low-Carbon Steel/Ni-Cr-W Alloy Bimetallic Material via Liquid–Solid Compound Casting with a Laser Assisted Solid Surface. *Machines* **2024**, *12*, 522. https://doi.org/10.3390/machines12080522

Academic Editors: Angshuman Kapil and Abhay Sharma

Received: 1 July 2024
Revised: 26 July 2024
Accepted: 29 July 2024
Published: 31 July 2024

Copyright: © 2024 by the authors. Licensee MDPI, Basel, Switzerland. This article is an open access article distributed under the terms and conditions of the Creative Commons Attribution (CC BY) license (https://creativecommons.org/licenses/by/4.0/).

1. Introduction

In the field of metal engineering, there is an increasing demand for castings with better mechanical and special properties, such as resistance to abrasive wear or resistance to corrosion at elevated temperatures [1–3]. Castings for this purpose are often manufactured entirely from expensive materials based on Ni, Co, Ti, or other alloying elements. But in many cases, high-performance properties are only necessary for the working surface layer of the molded components [4]. It is important to note that the wear limits of parts vary within a wide range, depending on a number of factors, and can vary from 100 to 200 μm to several mm. However, in practice, they do not exceed 5 mm.

There are several basic processes for manufacturing multilayer and bimetallic materials in the metal industry (Figure 1) [5–7], including gas flame, plasma, and detonation spraying, as well as vacuum and electrolytic deposition. These methods are known for their high productivity and the wide range of materials they are applicable to. In recent years, plasma technologies for the application of functional bilayer coatings have become significantly widespread, especially in the metallurgical industry. However, they have several substantial drawbacks: the adhesion strength of such coatings to the base material does not exceed

15–20 kg/mm^2; the thickness of high-quality coatings is limited; and they cannot be used for parts that operate under conditions of hydro-, gas-, and impact-abrasive wear or cyclic alternating loads [8–10].

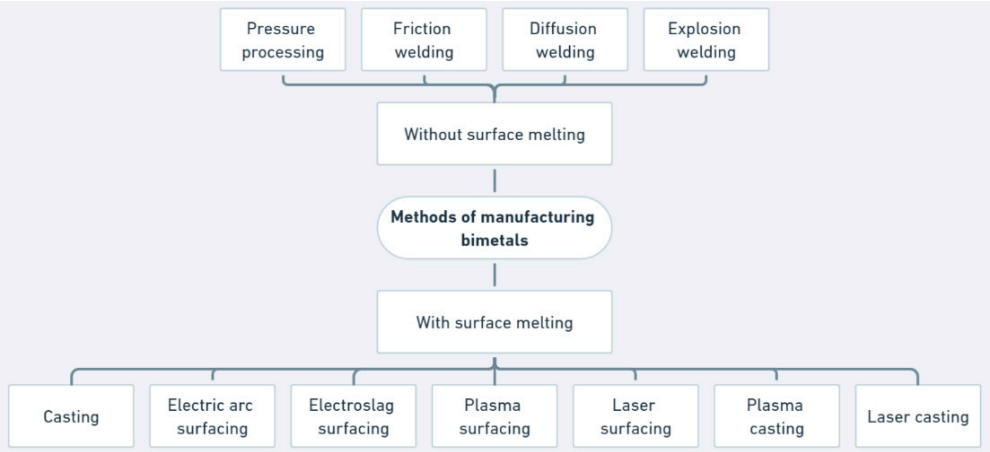


Figure 1. Methods for manufacturing bimetallic materials in industry.

The method of explosive welding for manufacturing bimetallic components is the most common in the industry for producing bimetals that include both homogeneous (alloyed, corrosion-resistant, heat-resistant, non-alloy steel) and heterogeneous (aluminum-copper, steel-copper) components. This process is characterized by a high productivity and strong adhesion between components due to diffusion processes, low production costs, a wide range of bimetals, and ease of production organization. However, it also has certain drawbacks such as a low process controllability and the uneven adhesion strength of bimetal components, especially over large areas, as well as high levels of noise and vibrations, which require additional protective measures [11,12].

One of the oldest and most cost-effective processes for producing layered metals is casting technology, which can be competitive with other widely used technologies such as cladding and thermal spraying [13–15]. Casting is popular because this technology not only provides economic benefits but also prevents the initiation and growth of a heat-affected zone, which can occur in the final products when other layering methods are applied. Numerous publications focus on innovations, technology enhancements, and the investigation of bimetallic material properties [16–18].

The research paper [19] talks about a new technology for bimetallic layered castings that uses a method of layering a coating directly in the casting process (method of mold cavity preparation). This is the cheapest way to improve the surfaces of castings because the element that will be the working surface layer of the casting is put into the mold as a solid or granular insert before the molten metal is poured in. Austenitic steel (X10CrNi 18-8 steel) forms the surface layer (working part) of prepared casting examples, while a typical foundry material (ferritic-pearlitic carbon-cast steel) forms the substrate (bearing part). The microstructure and mechanical properties of prepared bimetallic layered castings have been studied using metallography, non-destructive ultrasonic testing, and hardness testing. Studies have found that using a pouring temperature of 1650 °C and carbon-cast steel with a concentration of 0.6% on the bearing part of bimetallic layered casting makes it possible for this material to join well with alloy steel X10CrNi 18-8.

The study carried out in [18] investigates a very similar process for manufacturing bimetallic castings from pearlitic gray cast iron and different alloy steels [20] (high chromium steel X16Cr13, chromium-nickel austenitic steel X10CrNi18-8, or duplex ferritic-austenitic steel X2CrNiMoN22-5-3). The steel part is placed in the casting mold just before the pearlitic gray cast iron, which forms the bearing part, is poured. In this case, steel plates with a thickness of 5 mm were used, and the surfaces that were in contact with the molten metal were covered with an activator in the form of boron and sodium. These compounds facilitate

the formation of a bimetallic joint. The thickness ratio between the bearing and working parts is about 8:1. The proposed founding technology, which is based on a mold cavity preparation method, enables the creation of bimetallic layered castings in various configurations. These configurations include a bearing part made of pearlitic gray cast iron, a working part (layer) made of high-chromium ferritic or martensitic alloy steel, or a chromium–nickel austenitic or duplex ferritic–austenitic alloy. Furthermore, these castings are free from defects, particularly in the sensitive area of the joint between both materials. The permanent joint that was made between the steel plate and the gray cast iron is characterized by diffusion, which is mostly caused by carbon moving from the cast iron to the steel.

One publication [21] has studied the possibility of obtaining bimetals through continuous horizontal casting when the composition of components occurs in a liquid state without mixing. Binary mixtures of the eutectic-type bimetals Al-Zn, Al-Sn, and Al-Pb were selected, and contact layers of the composite metals were investigated using metallographic, X-ray diffraction, microscopic, and ultrasonic analyses. It was established that the size of the diffusion zone of the interface layer for the production of bimetallic compositions through the direct connection of liquid-phase components was 0.1–0.5 mm.

Despite the achievements in [18–23], manufacturing high-quality bimetallic products using this method is a difficult task in practice. In this case, the bonding of bimetal layers occurs after pouring, which leads to the formation of oxide films that can worsen the adherence of the layers.

Methods to modify the surface of solid substrates significantly impact the structure and mechanical properties of bimetallic materials.

Laser treatment is used to create a regular macroroughness on the substrate's surface. This promotes better adhesion between the metal layers by altering the structure and increasing the number of grain boundaries and defects, which enhances the diffusion of elements between the layers. It significantly influences mechanical properties by improving the adhesion and wear resistance of the materials [24].

Explosive welding is used to join two metals through an explosion, causing plastic deformation and welding. It forms a wavy structure at the boundary between the layers, which improves mechanical stability. This method affects the mechanical properties of the alloys by increasing adhesion strength and resisting delamination [11].

Plasma spraying allows for the creation of high-quality coatings with various properties. Its structure ensures a uniform distribution of particles and micropores. This process also changes mechanical properties, increasing hardness and wear resistance, but may reduce impact toughness [25].

The primary aim of this study is to enhance the process of manufacturing bimetallic materials by combining laser treatment with traditional casting methods to achieve superior mechanical and structural properties. This research focuses on optimizing the process parameters, including the melt-to-solid phase ratios and pouring temperatures, to produce high-quality bimetallic castings with improved thermal, corrosion, and wear resistance. As part of the experiment, alloy-grade nickel UNS 6230 plates are treated with a laser to make a regular macro-relief on their surface.

2. Materials

The bimetallic castings were fabricated and consisted of two main parts: the base (bearing part) and the (working part) surface layer. The bearing part of the bimetallic casting was a typical and widely used material for foundry production—non-alloy structural steel S235JRG2—whereas the working layer was made from a plate of nickel-based alloy of grade UNS 6230 [26–30]. Alloy 6230, a nickel–chromium–tungsten–molybdenum alloy, is well known for its excellent high-temperature strength, long-term stability, resistance to oxidizing environments up to 1150 °C, creep and fatigue resistance at high temperatures due to its lower thermal expansion characteristics, and fabricability at room temperature. The chemical compositions and physical and mechanical properties of the materials used are shown in Tables 1–3 [31,32].

Table 1. Chemical composition of materials.

Material	C	Si	Mn	Cr	Ni	Mo	W	Cu	Ti	Co	B	Fe	Al	P	S
UNS 6230	Max 0.05–0.15	Max 0.25–0.75	0.3–1.0	20.0–24.00	Rest	Max 1.0–3.0	13.0–15.0	Max 0.5	Max 0.1	Max 5.0	Max 0.015	Max 3.0	0.2–0.5	Max 0.25–0/75	Max 0.015
Steel S235JRG2 according EN 10250-2	Max 0.2	Max 0.55	Max 1.4	Max 0.3	Max 0.3	Max 0.08	-	-	-	-	-	Rest	Min 0.02	Max 0.045	Max 0.045

Table 2. Physical properties of applied materials.

Material	Density, g/cm^3	Melting Point, °C	Specific Heat, J/kg °C	Coefficient of Expansion, 20–100 °C, µm/m °C	Thermal Conductivity, W/m °C	Hardness, HB
S235JRG2	7.85	1420–1460	461	31	32	Max 334
UNS 6230	8.97	1301–1371	397	12.7	8.9	Max 241

Table 3. Mechanical properties of the applied materials.

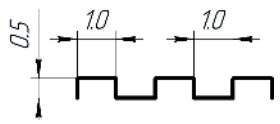
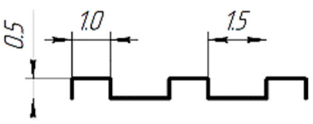
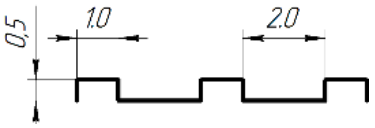
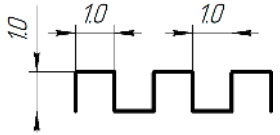
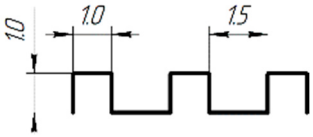
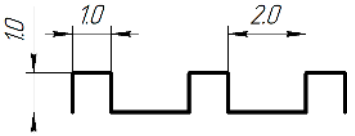
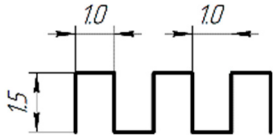
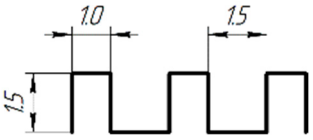
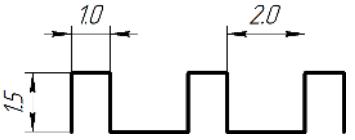
Material	Relative Elongation, %	Modulus of Elasticity, E [GPa]	Shear Modulus, G [GPa]	Yield Strength, $\sigma_{0.2}$ [MPa]	Ultimate Strength, σ_B [MPa]	Poisson's Ratio ν	Strength Coefficient E_1 [GPa]
S235JRG2	21–24	200	80	235	340–470	0.29	0.512
UNS 6230	40	210	79	Min 345	Min 760	0.31	1.52

3. Methodology for Bimetal Manufacturing

To apply a regular macro-relief to the surface of the plates of the functional material with dimensions of 100 × 50 × 4 mm, the technological laser complex Aramis LTC75 (Ukraine) was used. Process parameters: P = 400–500 W, S = 1–2 m/min, p = 2–3 atm, d = 0.4–0.5 mm.

On the surface of the plates, a regular macro-relief in the form of square-shaped protrusions with cross dimensions of 1 × 1 mm was fabricated through radiation with a fiber laser in the evaporation mode, combined with mechanical processing. The height of the protrusions on all samples was h = 0.5; 1.0; 1.5 mm, with the spacing between protrusions along two coordinates being 1.0; 1.5, and 2.0 mm (Table 4). The height and spacing between the protrusions were chosen based on previous research. FEA modeling showed that these protrusion arrangements are optimal for the uniform distribution of temperature in the functional layer due to the contact area, based on the size, area, and configuration of the protrusions themselves [33].

Table 4. Scheme of the macro-relief in the form of square-shaped protrusions with cross dimensions of 1 × 1 mm on the plates.

Height \ Spacing	1.0	1.5	2.0
0.5			
1.0			
1.5			

The melted structural component, grade S235JRG2 steel, was poured into a sand mold where plates made of nickel alloy UNS 6230, treated on the pouring side, were fixed.

Green sand was used in the mold, which is a mixture of silica sand, clay (bentonite), and water. This type of mold was chosen for its ease of preparation and low cost. Green sand has a high moisture content, which allows it to retain shape when filled with molten metal, and it also has a good thermal stability. Additionally, a graphite coating was utilized as a molding layer due to its favorable properties and relatively low cost.

The melt temperature was maintained at 1600 °C, as measured by a tungsten–rhenium thermocouple. To ensure sufficient thermal conductivity and mold stability during the pouring of the molten metal, the mold was preheated in a drying oven at 300 °C for 4 h. After the pouring process was completed, the samples and the mold were cooled for 4 h until the mold and the castings reached room temperature (20 °C). Gradual cooling minimizes internal stresses in the material, reduces the risk of cracks or other defects, and ensures the dimensional stability of the obtained bimetallic blanks.

Technological and schematic view of the bimetallic casting process.

Samples made of nickel alloy were placed in a sand mold (Figure 2), after which they were heated to a temperature of 300 °C and maintained in the furnace for 3 h. The melted structural component of the bimetal, steel S235JRG2, preheated to a temperature of 1600 °C, was applied to the surface of the samples through a separate gating system. After casting,

the samples and the mold were cooled for 4 h. The carbon concentration in the S235JRG2 steel was 0.30 wt%.

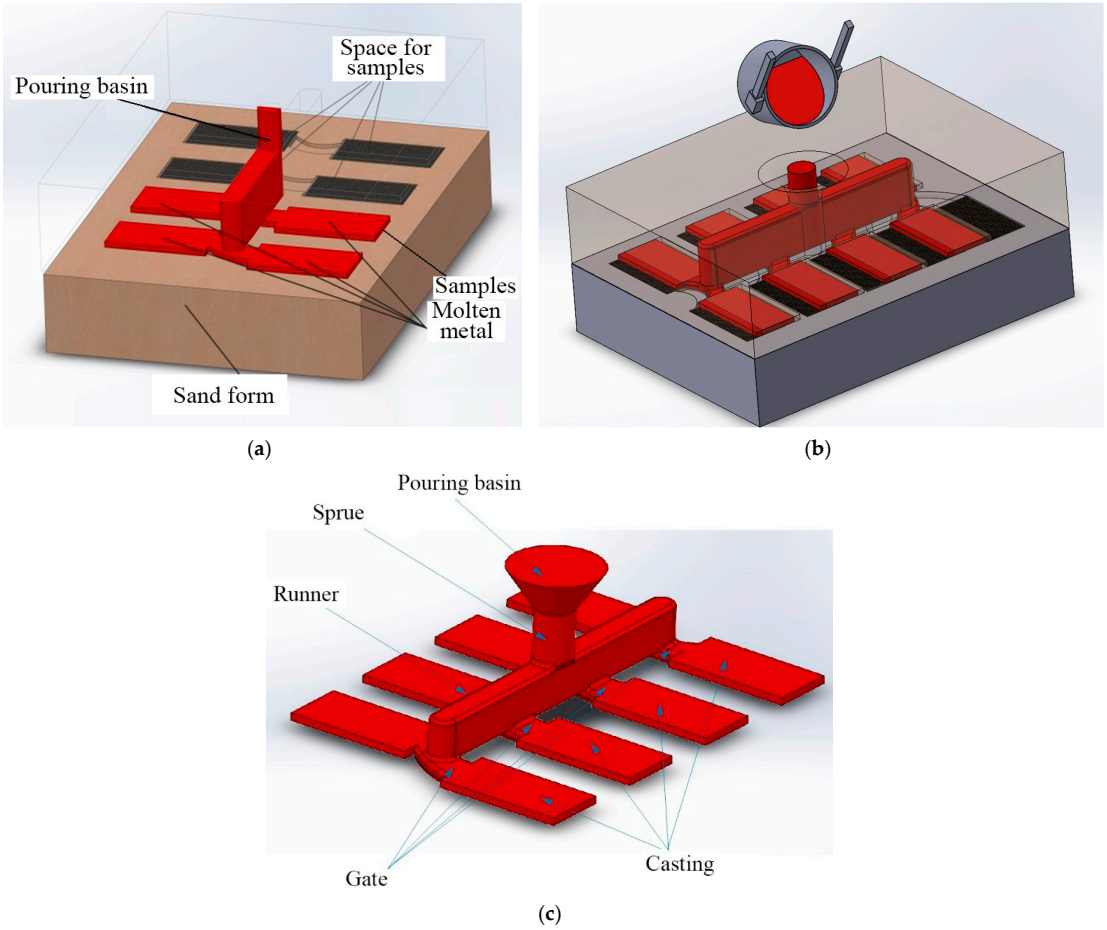


Figure 2. Schematic of the bimetallic casting process: (**a**) sand casting system components; (**b**) cross-section view; (**c**) gating system design.

The principles for reducing turbulence are a smooth flow, adequate sprue height, and optimized gate design. They should also be tapered to reduce pressure and turbulence. The non-pressurized gating system consists of (Figure 2c) a sprue (area 40 × 30 mm), runner (area 280 × 30 × 22 mm), ingates (area 6 × 30 mm).

4. Methodology for Samples Analysis

For the microstructure analysis, all specimens were cut using the EDM method. The primary cutting line was a vertical cut along the center of the 100 mm length. In addition, smaller sections were cut off both sides near the central part.

To reveal the microstructure, microsection samples were prepared, which were subjected to etching with a specialized "Murakami" solution and a 3% solution of nitric acid in ethyl alcohol. Subsequently, the microsections were rinsed with water and alcohol and dried with filter paper.

To determine the phase composition of the obtained bimetals, X-ray diffraction analysis was conducted using the "Theta-2-Theta" method on a Rigaku Ultima IV X-ray diffractometer with a graphite monochromator in copper radiation CuKα = 0.15418 nm (Rigaku Corp., Tokyo, Japan). Voltage: 30 kV; current strength: 30 mA; slit width that limits the X-ray beam: 6 mm. In the study, the Bragg–Brentano focusing scheme was used. Research conditions: angle range 2-Theta = 25–140°; shooting step—0.04°; exposure time at point—2 s; duration of shooting one sample—90 min.

An analysis of the obtained X-ray spectra and quantitative and qualitative phase analyses were performed using the PDXL software (version 2.9), the International Centre for Diffraction Data (ICDD, PDF-2), and the open Crystallographic Data Database (COD).

The features of the formation of the joining zone of bimetal components were studied using an REM-106I (Ukraine) scanning electron microscope with an energy-dispersive microanalysis system (EDX). The main characteristics of the device include the following: vacuum up to 5×10^{-6} mm Hg; accelerating voltage from 0.5 to 30 kV; resolution in secondary electrons in high vacuum mode: 4 nm; and in low vacuum mode: 6 nm; tungsten (W) cathode.

The investigation of the physical and mechanical properties of the bimetal samples was conducted using the "Micron-Gamma" device (Ukraine) using the continuous indentation method with a diamond indenter under a load of 50 gf and automatic fixation of its penetration depth. The loading rate was 5 gf/s. On each sample, 15 measurements were performed with a step of 100 μm between the indents of the indenter.

Analysis and processing of indentation diagrams for determining microhardness were performed automatically using the device software, based on the Oliver and Pharr method, which is accepted as an international standard.

5. Results and Discussions

On the surface of the plates, the laser radiation created a macro-relief with cross dimensions of 1 × 1 mm and different heights and spacings based on Table 4. The real samples are presented in Table 5. Then, the samples were prepared for the casting process based on the procedure mentioned in Section 3.

Table 5. Macro-relief in the form of square-shaped protrusions on the real samples.

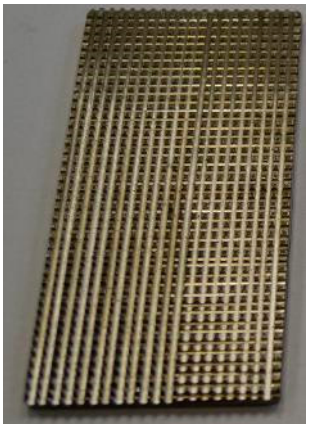
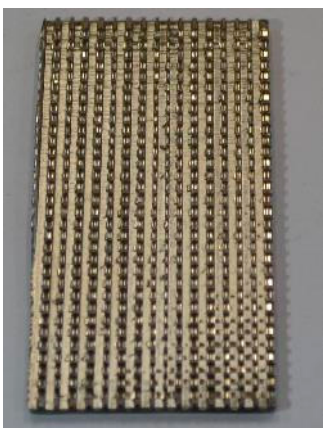
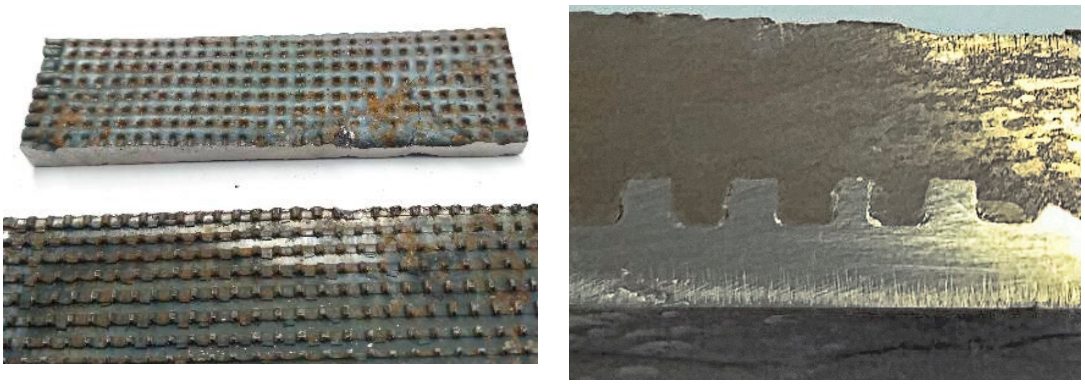
Height \ Spacing	1.05	1.5	2.0
0.5			
1.0			

Table 5. *Cont.*

Height \ Spacing	1.05	1.5	2.0
1.5			
			1000µm

Following preliminary mechanical tests, it was found that some samples had delaminated and were excluded from further studies. Specifically, samples with dimensions of 1 × 0.5 h; 1 × 1.0 h; 1.5 × 1.0 h; 2 × 0.5 h, and 2 × 1.0 h—which constituted about 55% of the total number—had completely delaminated. Infiltration and encapsulation of the protrusions of the applied structure were observed (Figures 3 and 4). Areas where S235JRG2 melt did not mix were those where the temperature was not sufficient for infiltration due to high heat dissipation in the area of interaction between the two environments.

Microanalysis of samples 1 × 1.5 h, 1.5 × 1.5 h, and 2 × 1.5 h showed that the casting side had some mechanical bonding and that there were individual contact zones with metallurgical bonding. The ratio of the contact area to the total did not exceed 10–15% (Figure 5).



(**a**) (**b**)

Figure 3. Main view samples after the casting process: (**a**) before and after the casting process, sample 1 × 0.5 h; (**b**) a cross-section view, sample 2 × 1.5 h.

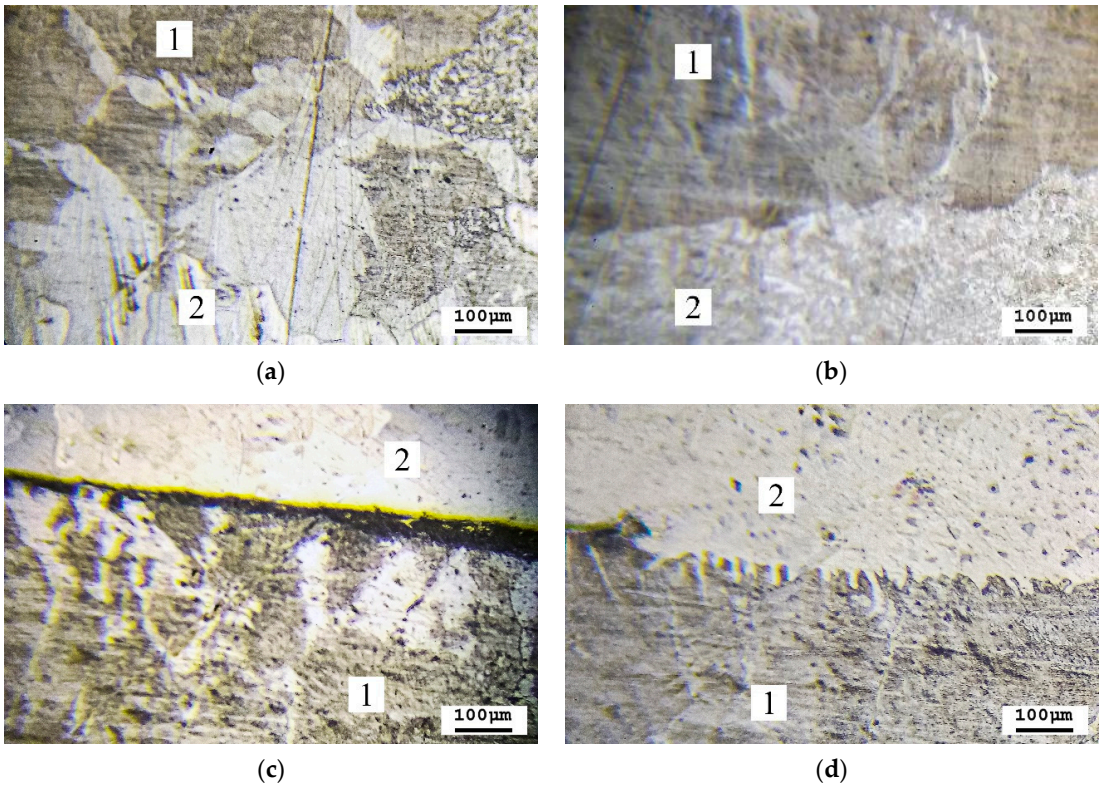


Figure 4. Analysis of samples after the casting process: (**a**) sample 1.5 × 0.5 h; (**b**) sample 1.5 × 0.5 h; (**c**) sample 1 × 1.5 h; (**d**) sample 2 × 1.5 h. 1—Steel S235JRG2; 2—UNS 6230.

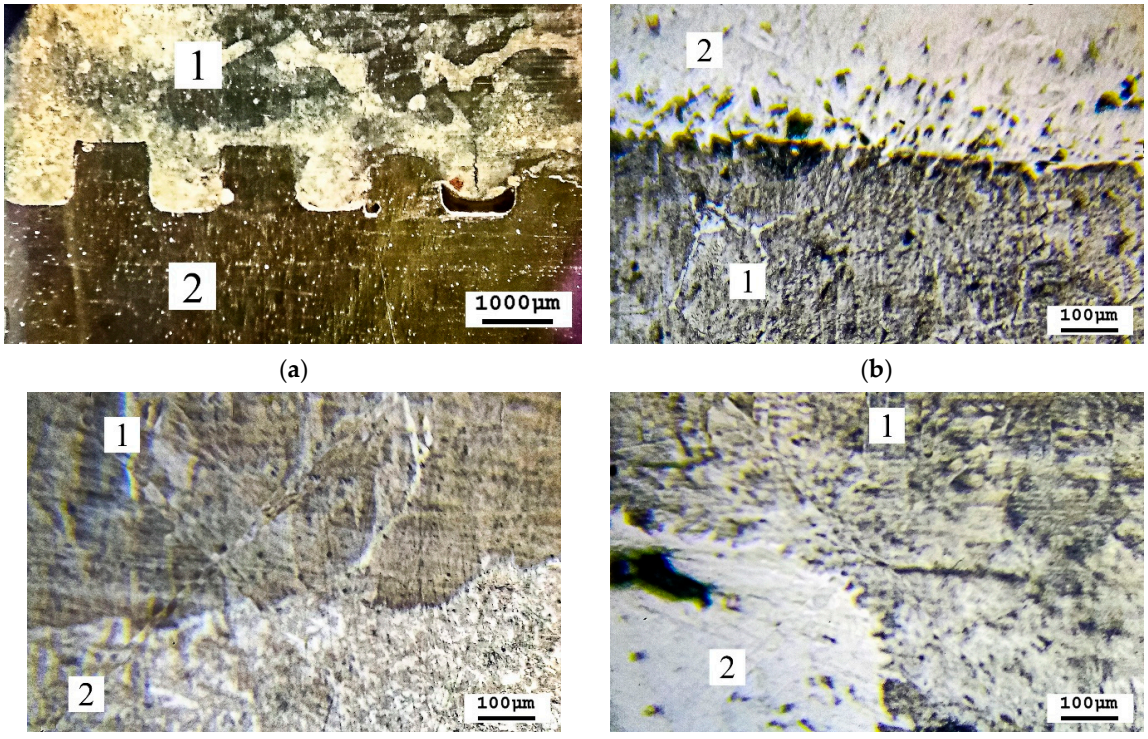


Figure 5. Analysis of samples with a height of 1.5 and spacing of 1.0 after the casting process: (**a**) main view; (**b**,**c**) enlarged view of the bimetallic area; (**d**) enlarged view of the corner. 1—Steel S235JRG2; 2—UNS 6230.

Figure 6 presents the microstructures of the obtained bimetallic two-layer castings. During the microanalysis of sections from the 1.5 × 0.5 h sample, a stable formation was detected in the contact zone of the molten steel S235JRG2 with the nickel alloy UNS 6230. The protrusions had a height of 0.5 mm, and they were positioned at a 1.5 mm interval. The contact area's ratio to zones where a metallurgical bond is observed (the boundary lacks a separation zone) exceeded 85% across the entire bonding boundary.

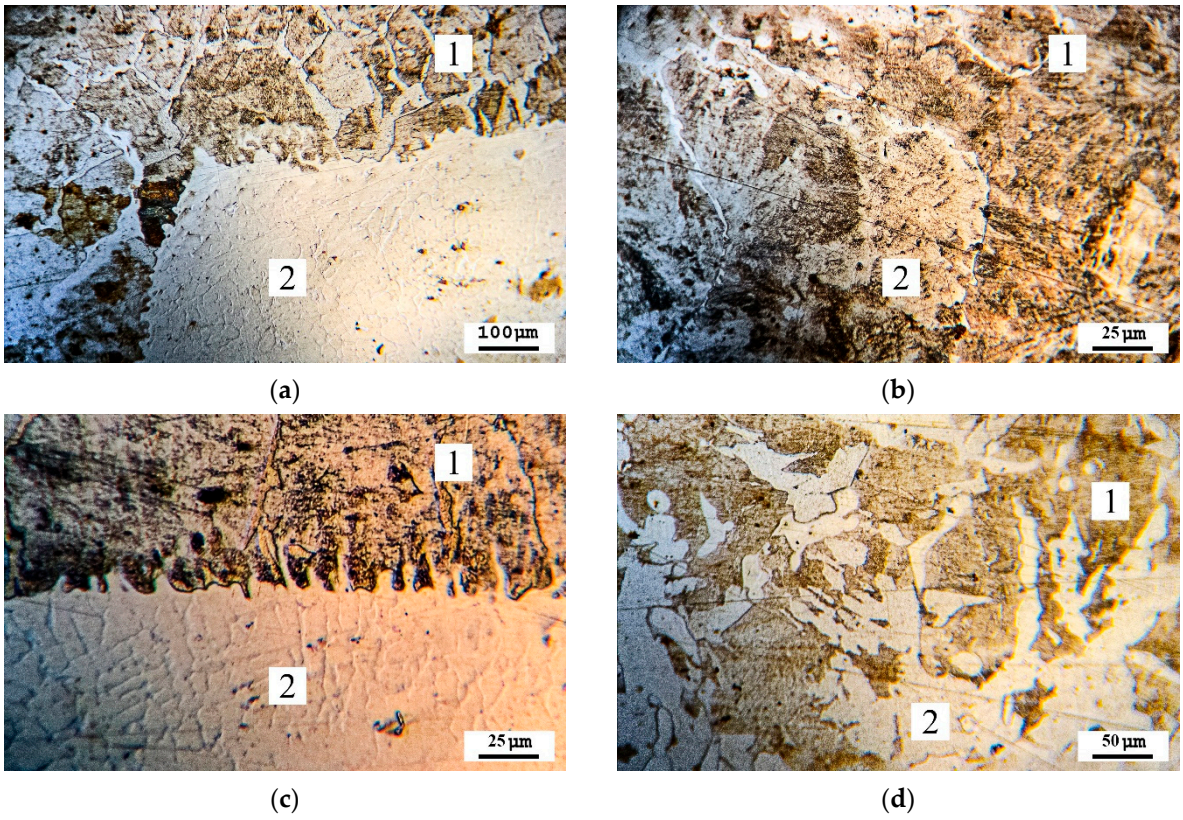


Figure 6. Microstructure of bimetallic samples double-layer castings: (**a**) main view; (**b**) enlarged Steel S235JRG2 area; (**c**) transition zone; (**d**) enlarged view of transition zone. 1—Steel S235JRG2; 2—UNS 6230.

As a result of the diffusion of carbon and alloying elements such as Cr, Ni, and W, a transition zone was formed at the boundary between the carbon steel S235JRG2 and the plate made of the nickel alloy (UNS 6230). The width of this melting zone varied from 80 to 170 µm. The shape of the transition zone structurally differed from S235JRG2 and UNS 6230 which clearly indicates the diffusion process (Figure 5).

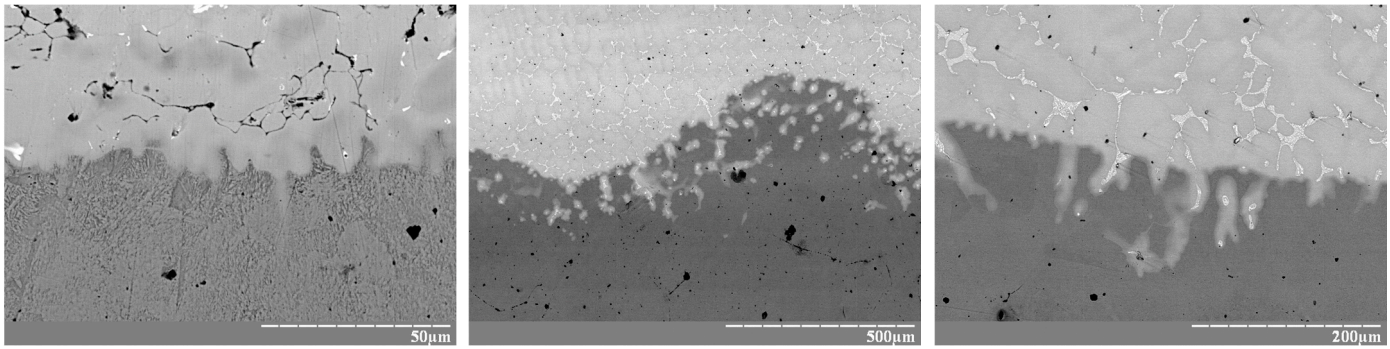
Interlayer diffusion is the process in which atoms of one material move into another material across the interface. In the case of bimetals such as Ni, Cr, W, Fe, and C, this process affects the microstructure and mechanical properties of the final product.

The diffusion mechanisms in Ni, Cr, W, Fe, and C can be explained by processes in high entropy alloys, where each atom of the constituent elements has an equal probability of occupying a lattice site. Due to the heterogeneity of the atoms, the potential energy between the lattice sites varies. Fluctuations in the potential energy of interatomic bonds significantly affect the kinetics of diffusion and its activation energy [34]. Nickel aids in the stabilization of austenite, while tungsten has a low diffusion capability. In the bimetal's interfacial zone, carbides like tungsten carbide (WC) and Cr_3C_2, Fe_3C, WC, and Ni_3C do not form. This improves the properties of the transition layer, as these phases can act as potential stress concentrators under cyclic loading or fatigue, leading to cracks and defects during further operation. The absence of carbides is also confirmed by the microhardness

measurements, which show a smooth variation and indicate the absence of points with increased microhardness [35].

Phase formation processes for Ni-Cr-Fe and Fe-Ni are complex and depend on several thermodynamic and kinetic factors [36]. Diffusion occurs through vacancies and interstitial positions in the crystal lattice and depends on temperature and concentration gradients [37].

Based on the results of SEM microscopy (Figure 7), it can be concluded that the protrusions on the functional component almost completely melted, resulting in the formation of a solution of the nickel alloy in the carbon steel. The boundary of separation is blurred and has a wavy shape, which is due to the geometry of the protrusions that were on the surface of the nickel alloy prior to interaction with the melt. On samples with protrusions that had a greater height (1 mm), the waviness of the melting zones has a larger amplitude, to some extent replicating the profiles of the protrusions. However, this sample had a low bonding area, not exceeding 20%, due to the insufficient temperature in the transition zone and high cooling rates.



(**a**) (**b**) (**c**)

Figure 7. SEM microscopic examinations, samples: (**a**) 2.0 × 1.5 h; (**b**) 1.5 × 1.0 h; (**c**) 1.5 × 0.5 h.

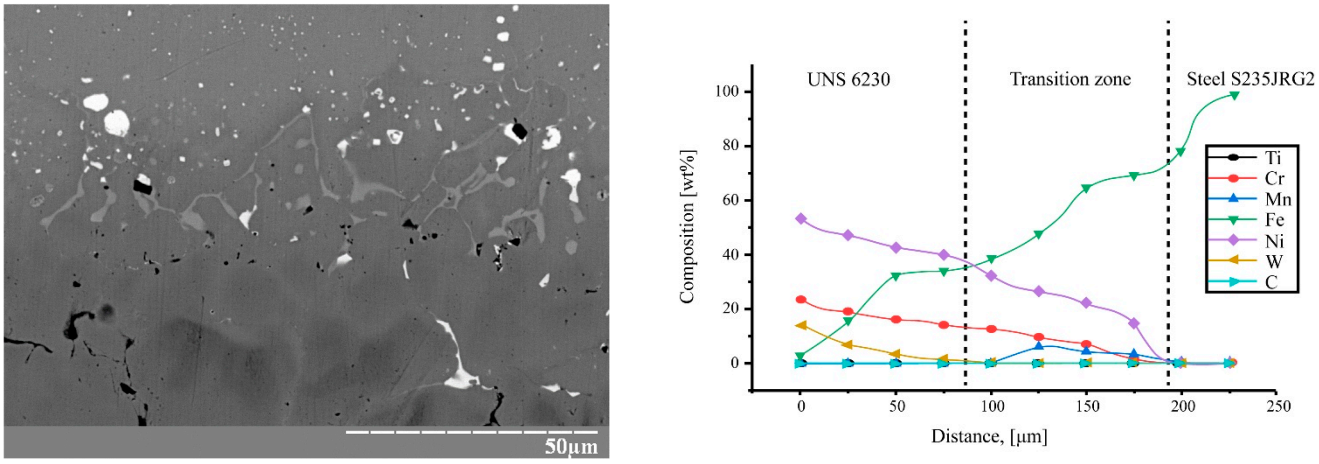
For the 1.5 × 0.5 h sample, the ratio of the contact areas with zones where metallurgical bonding occurred was the highest, accounting for 97–98%; for 2 × 1.5 h it was 25–30%. In the microstructural images, two layers are clearly visible. The upper layer, whose microstructure is practically indiscernible when treated with standard reagents, belongs to the nickel alloy. This layer is adjacent to the ferrite–pearlite structure of the carbon steel S235JRG2.

Upon further magnification, clusters of white-colored grains of various sizes became visible at the boundary between these structures and in certain areas of them. These regions also resist etching poorly and have a higher content of Cr, Ni, and W.

In addition to optical metallography, structural studies were conducted using elemental chemical microanalysis with a scanning electron microscope equipped with a micro-X-ray spectroscopic attachment (Figures 8 and 9; Tables 6 and 7).

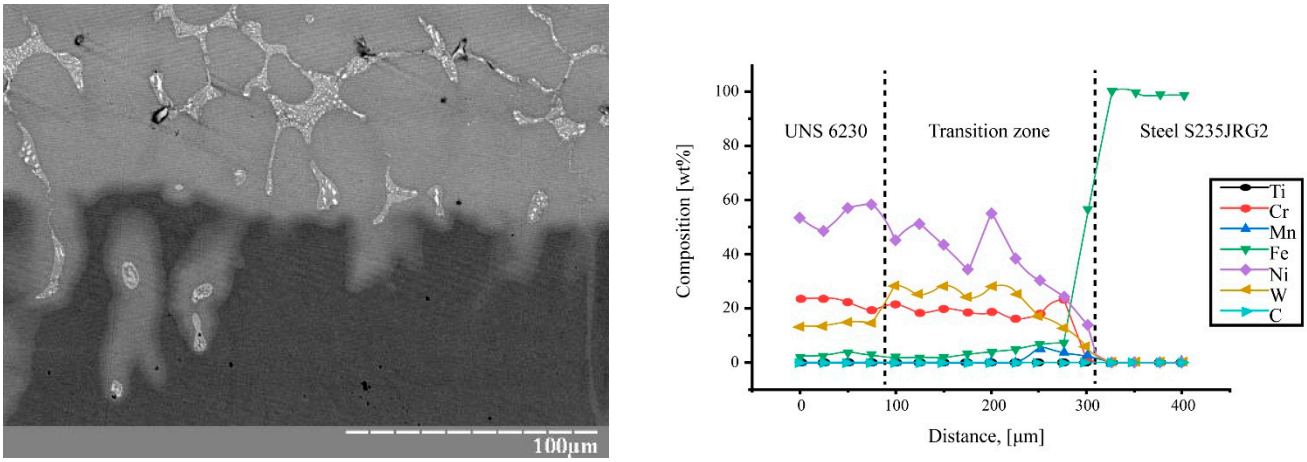
Table 6. The content of alloying elements in different areas of the fusion zone between the nickel alloy UNS 6230 and steel S235JRG2 (bxh = (2 × 1.5) mm).

	Ti	Cr	Fe	Ni	W	Bimetal Layer
1	0.09	23	2.92	56.9	14.10	UNS 6230
2	0.08	18.49	36.75	42.08	3.40	Transitional 4
3	0.07	16.87	46.96	30.51	2.70	Transitional 3
4	0.04	10.94	68.83	21.50	1.90	Transitional 2
5	0.06	5.38	79.28	0.08	0.17	Transitional 1
6	0.02	0.06	99.76	0.05	0.10	S235JRG2



(**a**) (**b**)

Figure 8. SEM microscopic examinations (sample 2 × 1.5 h): (**a**) microstructure; (**b**) EDS analysis.



(**a**) (**b**)

Figure 9. SEM microscopic examinations (sample 1.5 × 0.5 h): (**a**) microstructure; (**b**) EDS analysis.

Table 7. The content of alloying elements in different areas of the fusion zone between the nickel alloy and steel S235JRG2 (bxh = (1.5 × 0.5) mm).

	Ti	Cr	Fe	Ni	W	Bimetal Layer
1	0.08	23.1	2.90	56.8	14	UNS 6230
2	0.06	24.0	4.12	46.46	16.52	Transitional 9
3	0.07	22.3	5.24	58.50	18.95	Transitional 8
4	0.05	20.13	3.61	60.64	17.63	Transitional 7
5	0.06	22.60	3.85	40.2	30.27	Transitional 6
6	0.05	20.08	4.02	52.3	25.6	Transitional 5
7	0.04	22.62	5.67	41.72	30.43	Transitional 4
8	0.02	21.26	7.35	33.62	24.29	Transitional 3
9	0.03	22.12	9.29	56.46	18.16	Transitional 2
10	0.01	2.60	11.01	15.64	4.93	Transitional 1
11	0	0.12	99.36	0.15	0.1	S235JRG2

X-ray phase analysis diffractograms of the transition zone, taken from the area of the bimetal's cross-section with a diameter of 6 mm, that were symmetrical and relative to the hypothetical line of connection, can be seen in Figure 10. The sample's transition layer had a macro-relief of 2 × 1.5 mm, and the bimetal parts were only fusing at a level of 20–30%

per area. The content of the NiCr–Fe phase constitutes 89.1%, and the Fe 0.507 Ni 0.493 (tetrataenite) phase constitutes 10.9%.

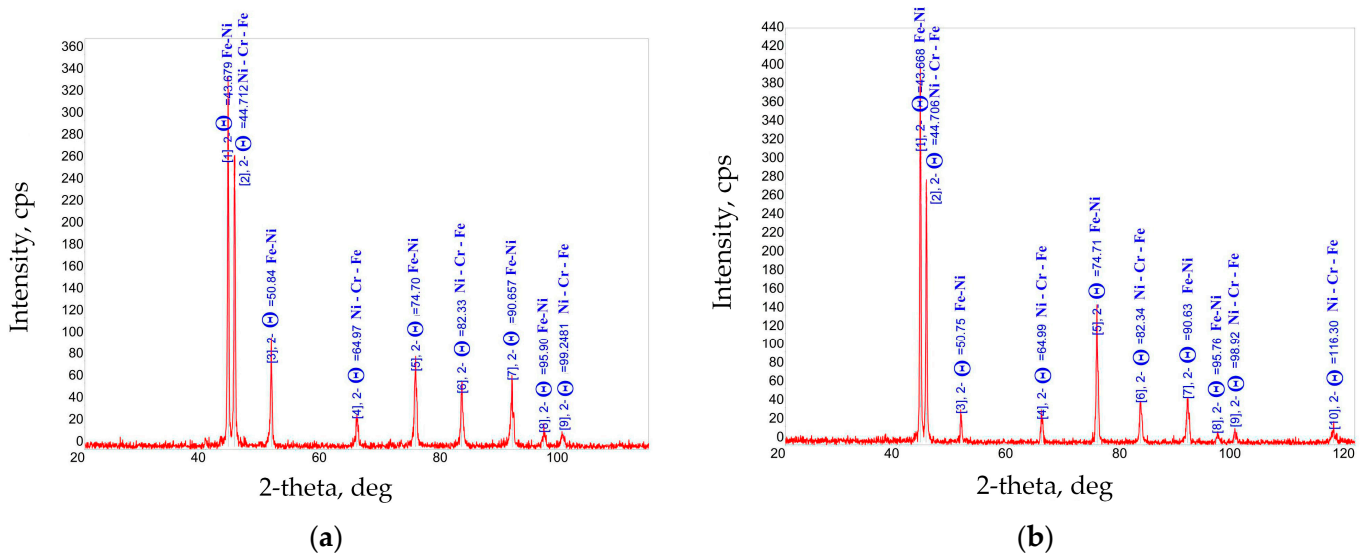


Figure 10. Diffraction patterns of the transition layer of the bimetal "nickel alloy-steel S235JRG2" with varying macro-relief: (**a**) sample 2 × 1.5 h mm.; (**b**) sample 1.5 × 0.5 h mm on the surface of the functional component of the alloy.

In the bimetal transition layer with the 1.5 × 0.5 mm parameters, when the content of the Ni-Cr-Fe phase in the fused layer amounted to 86.4%, the boundary of the fusion area was larger and the structure was more uniform. This is also evidenced by the increased in the Fe 0.507–Ni 0.493 phase (tetrataenite) to 13.6%.

The sample with a larger macro-relief (2 × 1.5 mm) had a smaller phase composition of Fe 0.507–Ni 0.493 (tetrataenite) in the transition layer, and the main phase was Ni-Cr-Fe. For the sample with a smaller macro-relief (1.5 × 0.5 mm), the phase composition of the transition layer was larger, and an increase in the content of the Fe 0.507–Ni 0.493 (tetrataenite) phase was also observed—this could be due to a faster cooling rate in the first case, as the area of heat dissipation is larger under identical conditions of casting with the liquid base phase.

On the sections of bimetal samples, the functional component of which had a macro-relief of 1.5 × 0.5 mm, the distribution of the microhardness was determined in the direction perpendicular to the bonding zone from the surface to the carbon steel under a load of 50 g. Figure 11 presents the results of the microhardness measurements, which show a sufficiently smooth decrease from 5 to 7 GPa in the nickel alloy to 4–5 GPa in the fusion zone and 3–4 GPa in the carbon steel.

Such a smooth decrease in microhardness in the fusion zone when transitioning from the nickel alloy to S235JRG2 indicates the distribution and mixing of the bimetal components, which affects the mechanical properties of the transition zone. Not only the magnitude of microhardness but also its distribution in depth indicate changes in microstructure and mechanical properties along the cross-section of the sample.

It was found that, with a macroscopic structure ratio and an increased interval to height at the same pouring temperature of 1600 °C (sample 2 × 1.5 h mm; sample 1.5 × 0.5 h), the solid phase in the melt leads to the formation of a more uniform microstructure, reducing the grain size and decreasing the number of defects in the material. This positively affects the mechanical properties, increasing the hardness and strength of the bimetal's transition layer. The main focus was on achieving a transition layer where alloying elements diffuse from one component to another, forming a transition layer with mechanical properties that

ensure a high-strength bond between the bimetal components and minimize the formation of defects and cracks during the subsequent operation of the products.

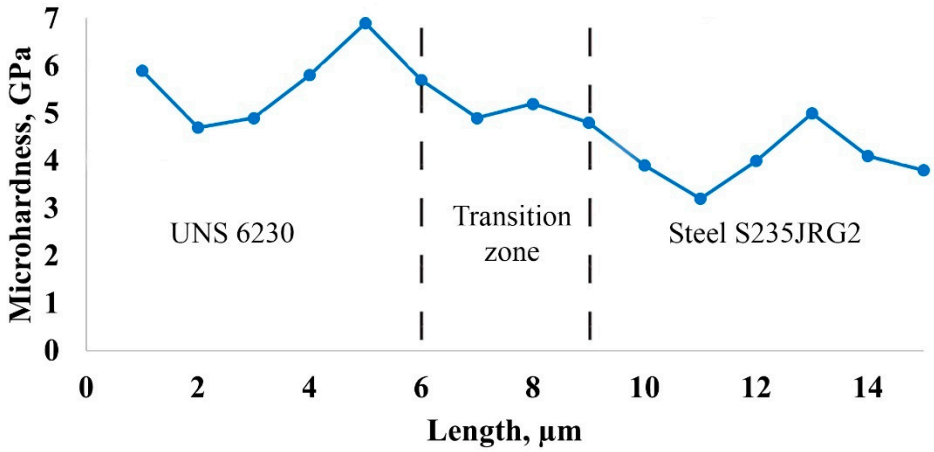


Figure 11. Distribution of microhardness across the fusion zone of the nickel alloy and carbon steel S235JRG2.

Overall, the transition layer is homogeneous and characterized by the presence of phases, which, during further operation, will prevent the concentration of internal stresses, which will positively affect the mechanical characteristics of the casting as a whole in the future.

The new technology, which combines pre-laser treatment with traditional casting methods, is highly efficient and will have broad applications across various industries as it achieves high levels of productivity, quality, and reliability. The developed technology enables the production of a variety of bimetallic combinations tailored to specific needs, significantly expanding its application.

The material exhibits improved mechanical properties. The regular macroroughness created by laser treatment on the surface during the casting process enhances the levels of adhesion between the layers (due to diffusion) and improves mechanical properties. This is particularly important for the oil, chemical, and heavy industries, where functional components are exposed to aggressive environments at high temperatures. As a result, parts can operate longer without significant defects, reducing maintenance costs and equipment downtime.

Enhanced Microstructure: Optimizing the ratio of the melt phase to the solid phase, as well as the pouring temperature, creates a more uniform and robust structure with a better distribution of alloying elements between the layers.

Microscopic studies revealed numerous formations near the fusion site. It was also noted that the obtained structure has a heterogeneous density of alloying elements, with their concentrations highest in the area of dissolution and diffusion in the transition zone. Furthermore, the chemical composition analysis showed that new phases had formed in the area under investigation.

Comparison with Existing Technologies:

Explosive Welding: Although it is known for its high productivity, explosive welding has low controllability and quality, especially in large areas. The new technology offers more precise process control, resulting in a higher product quality with equal or even greater productivity. Explosive welding generates high levels of noise and vibration, which require significant safety measures to be put in place. The new technology is safer and more environmentally friendly. Additionally, explosive welding can result in a less uniform microstructure and weaker bonds, particularly over large areas. The new technology addresses these issues, providing a more reliable and stable product.

Thermal Spraying: Thermal spraying methods often have a low adhesion strength, limiting their use under high loads. The new technology ensures stronger bonds between

layers, increasing the durability and performance of the final product. Thermal spraying is not suitable for parts subjected to cyclic loads because of the risk of delamination.

Metallographic studies have established the conditions under which a metallurgical bond is formed between the bimetallic components, ensuring the high strength of their connection. It was proven that to achieve high strength of the bimetal components' connection and an even distribution of this strength across the bonding plane, the height of the macro-protrusions and their pitch must have optimal dimensions.

6. Conclusions

A new efficient process for manufacturing bimetals was developed based on the applied laser as an assistive tool for substrate surface modification and the energy of the molten base component, provided by an induction source. An original scheme for its organization was proposed, according to which laser radiation is used to form a regular macro-relief with protrusions of respective configurations on the surface of the functional component. A diffusion transition layer is formed as a result of the interaction between the two environments, and the base melt is applied to this macro-relief. This layer is characterized by a reliable bond across the entire boundary and a smooth gradient of properties.

New phases appear in the bonding zone, including 86.4% of the Ni–Cr–Fe phase and phases Fe 0.507–Ni 0.493 (tetrataenite).

It was proven that, to ensure high strength of the bimetal components' bonding and an even distribution of this strength across the bonding plane, the height of the macro-protrusions and their pitch must have optimal dimensions. In the case of transverse dimensions of protrusions (1 × 1) mm, the optimal dimensions are 0.5 mm for the height of the protrusions and 1.5 mm for the pitch between them.

The key parameters that are most critical when manufacturing bimetallic products using the new technology are the pouring temperature of the melt (controlled by heating in an induction furnace) and the interval/height of the applied macroroughness (managed through laser dimensional treatment).

The intensification of the bimetal manufacturing process through the use of plastic deformation for the rapid application of a regular macrostructure on the surface of the functional component will significantly increase the process' productivity and is relevant for mass production.

These results indicate significant prospects for the use of manufactured bimetallic composites such as UNS 6230/S235JRG2, as well as their potential application in various fields where improved mechanical properties and durability are required.

Author Contributions: Conceptualization, L.G. and S.S.; methodology, S.S.; validation, S.S., L.G. and O.K. (Oleksii Kaglyak); investigation, S.S. and O.K. (Oleksii Kaglyak); writing—original draft preparation, S.S., O.K. (Oleksandr Kapustynskyi) and N.V.; writing—review and editing, N.V. and O.K. (Oleksandr Kapustynskyi); visualization, O.K. (Oleksandr Kapustynskyi); supervision, S.S. and N.V. All authors have read and agreed to the published version of the manuscript.

Funding: This research received no external funding.

Data Availability Statement: The original contributions presented in the study are included in the article, further inquiries can be directed to the corresponding author.

Conflicts of Interest: The authors declare no conflicts of interest.

References

1. Ramadan, M. Interface Characterization of Bimetallic Casting with a 304 Stainless Steel Surface Layer and a Gray Cast Iron Base. *Adv. Mater. Res.* **2015**, *1120–1121*, 993–998. [CrossRef]
2. Wang, D.; Sun, X.; Jiang, Y.; Chang, X.; Yonglei, X. Review on the application of stainless-clad bimetallic steel in the marine environment. *Anti-Corros. Methods Mater.* **2024**, *71*, 132–142. [CrossRef]
3. Mnif, R.; Baccouch, Z.; Elleuch, R.; Richard, C. Investigations of high temperature wear mechanisms for tool steel under open-sliding contact. *J. Mater. Eng. Perform.* **2014**, *23*, 2864–2870. [CrossRef]

4. Wróbel, T. Characterization of Bimetallic Castings with an Austenitic Working Surface Layer and an Unalloyed Cast Steel Base. *J. Mater. Eng. Perform.* **2014**, *23*, 1711–1717. [CrossRef]
5. Bandyopadhyay, A.; Zhang, Y.; Onuike, B. Additive Manufacturing of Bimetallic Structures. *Virtual Phys. Prototyp.* **2022**, *17*, 256–294. [CrossRef]
6. Gradl, P.; Tinker, D.C.; Park, A.; Mireles, O.R.; Garcia, M.; Wilkerson, R.; Mckinney, C. Robust metal additive manufacturing process selection and development for aerospace components. *J. Mater. Eng. Perform.* **2022**, *31*, 6013–6044. [CrossRef]
7. Ramadan, M.; Fathy, N.; Abdel Halim, K.S.; Alghamdi, A.S. New trends and advances in bi-metal casting technologies. *Int. J. Adv. Appl. Sci.* **2019**, *6*, 75–80. [CrossRef]
8. Davis, J.R. *Handbook of Thermal Spray Technology (Thermal Spray Technology)*; ASM International: Almere, The Netherlands, 2004.
9. Korzhyk, V.; Khaskin, V.; Ganushchak, O.; Strohonov, D.; Illiashenko, Y.; Fialko, N.; Guo, C.; Grynyuk, A.; Peleshenko, S.; Aloshyn, A. Features of structure formation when surfacing steel (iron) on titanium with plasma sprayed coatings in the technology of obtaining butt joint of bimetallic plates "titanium-steel". *East.-Eur. J. Enterp. Technol.* **2023**, *2*, 6–16. [CrossRef]
10. Li, B.; Fan, L.; Bai, J.; He, J.; Su, J.; Wang, S.; Deng, C.; Liu, S.; Zhang, Z. Study on porosity of thermal-sprayed commercially pure aluminum coating. *Materials* **2023**, *16*, 6612. [CrossRef]
11. Sherpa, B.B.; Rani, R. Advancements in explosive welding process for bimetallic material joining: A review. *J. Alloys Met. Syst.* **2024**, *6*, 100078. [CrossRef]
12. Sherpa, B.B.; Pal, D.K.; Batra, U.; Mishra, G.C.; Singh, B.B. Study of the Explosive Welding Process and Applications. In *Advances in Applied Physical and Chemical Sciences—A Sustainable Approach*; Excellent Publishing House: New York, NY, USA, 2014; pp. 33–39.
13. Fauchais, P.L.; Heberlein, J.V.; Boulos, M.I. *Thermal Spray Fundamentals*; Springer: Berlin/Heidelberg, Germany, 2014. [CrossRef]
14. Lehmhus, D. Advances in metal casting technology: A review of State of the art, challenges and trends—Part II: Technologies new and revived. *Metals* **2024**, *14*, 334. [CrossRef]
15. Ke, P.L.; Wu, Y.N.; Sun, C. Detonation gun sprayed thermal barrier coatings. In *Thermal Barrier Coatings*; Woodhead Publishing: Sawston, UK, 2011; pp. 175–189. [CrossRef]
16. Darabi, R.; Azodi, H.D.; Bagherzadeh, S. Investigation into the Effect of Material Properties and Arrangement of Each Layer on the Formability of Bimetallic Sheets. *J. Manuf. Process.* **2017**, *29*, 133–148. [CrossRef]
17. Shlyakhova, G.V.; Barannikova, S.A.; Bochkareva, A.V.; Li, Y.V.; Zuev, L.B. Structure of a Carbon Steel–Stainless Steel Bimetal. *Steel Transl.* **2018**, *48*, 219–223. [CrossRef]
18. Wróbel, T.; Szajnar, J. Bimetallic Casting: Ferritic Stainless Steel—Grey Cast Iron. *Arch. Met. Mater.* **2015**, *60*, 2361–2365. [CrossRef]
19. Wróbel, T.; Cholewa, M.; Tenerowicz, S. Bimetallic Layered Castings Alloy Steel—Carbon Cast Steel. *Arch. Foundry Eng.* **2011**, *11*, 105–107.
20. Wróbel, T.; Cholewa, M.; Tenerowicz, S. Bimetallic layer castings. *J. Achiev. Mater. Manuf. Eng.* **2010**, *43*, 385–392.
21. Marukovich, E.; Branovitsky, A.; Na, Y.-S.; Lee, J.-H.; Choi, K.-Y. Study on the Possibility of Continuous-Casting of Bimetallic Components in Condition of Direct Connection of Metals in a Liquid State. *Mater. Des.* **2005**, *27*, 1016–1026. [CrossRef]
22. Shapoval, O.; Drahobetskyi, V.V.; Savchenko, I.; Gurenko, A.; Markov, O.; Shapoval, A.A. Profitability of Production of Stainless Steel + Zirconium Metals Combination Adapters. *Key Eng. Mater.* **2020**, *864*, 285–291. [CrossRef]
23. Zhilin, S.G.; Komarov, O.N.; Bogdanova, N.A. Production of the Steel Casting with Improved Dimensional and Geometrical Accuracy Using Complex Models. *IOP Conf. Ser. Mater. Sci. Eng.* **2020**, *709*, 033104. [CrossRef]
24. Wen, K.; Zhang, G.; Zhang, Z.; Xue, S.; Bai, G.; Han, Y.; Xu, H. Enhanced bonding strength of Al/Fe bimetal by ni-based alloys ni-based interlayer prepared by laser cladding technique. *Mater. Today Commun.* **2024**, *38*, 107906. [CrossRef]
25. Wu, X.; Piñeiro-García, A.; Rafei, M.; Boulanger, N.; Canto-Aguilar, E.J.; Gracia-Espino, E. Scalable production of foam-like nickel–molybdenum coatings via plasma spraying as bifunctional electrocatalysts for water splitting. *Phys. Chem. Chem. Phys.* **2023**, *25*, 20794–20807. [CrossRef] [PubMed]
26. Han, Y.-B.; Xue, X.-Y.; Zhang, T.-B.; Hu, R.; Li, J.-S. Effects of hot compression on carbide precipitation behavior of ni—20cr—18w—1mo superalloy. *Trans. Nonferrous Met. Soc. China* **2016**, *26*, 2883–2891. [CrossRef]
27. Kim, D.; Sah, I.; Kim, D.; Ryu, W.-S.; Jang, C. High temperature oxidation behavior of alloy 617 and Haynes 230 in impurity-controlled helium environments. *Oxid. Met.* **2010**, *75*, 103–119. [CrossRef]
28. Rouillard, F.; Cabet, C.; Stéphane, G.; Wolski, K.; Pijolat, M. Mechanism of destruction of the protective oxide layer on Alloy 230 in the impure helium atmosphere of Very High Temperature Reactors. In Proceedings of the Eurocorr 2008 (The European Corrosion Congress), Edimbourg, UK, 7–11 September 2008.
29. Dudziak, T.; Witkowska, M.; Ratuszek, W.; Chruściel, K. XRD phase investigations of steam oxidized Fe and Ni rich Cr alloys. *Trans. Foundry Res. Inst.* **2017**, *57*, 265–276. [CrossRef]
30. Sas-Boca, I.M.; Frunza, D.I.; Ilutiu-Varvara, D.A.; Toma, I. The properties of bimetallic multi-layer (C45 and S235JR) and the multi-layer steel made by forging. *Powder Metall. Adv. Mater.* **2018**, *8*, 11. [CrossRef]
31. Special Metals. Available online: https://www.atimaterials.com/Products/Pages/ati-6230.aspx (accessed on 25 May 2024).
32. *EN 10250-2:2022*; Open Die Steel Forgings for General Engineering Purposes—Part 2: Non-Alloy Quality and Special Steels. European Committee for Standardization: Bruxelles, Belgium, 2022.
33. Salii, S.; Golovko, L.; Romanenko, V.; Bloshchytsyn, M. Research of the laser foundry process of manufacturing bimetals of different functional purposes. Beam technologies in welding and materials processing. In Proceedings of the Ninth International Conference, Odessa, Ukraine, 9–13 September 2019; pp. 100–102.

34. Durand, A.; Peng, L.; Laplanche, G.; Morris, J.; George, E.; Eggeler, G. Interdiffusion in Cr–Fe–Co–Ni medium-entropy alloys. *Intermetallics* **2020**, *122*, 106789. [CrossRef]
35. Raghavan, V. *Phase Diagrams of Binary Nickel Alloys*, 2nd ed.; Indian Institute of Metals: Kolkata, India, 2004.
36. Reed, R.C. *The Superalloys Fundamentals*; Cambridge University Press: Cambridge, UK, 2006. [CrossRef]
37. Berthod, P.; Aranda, L.; Podor, R.; Rapin, C.; Vébert, C. Study of carbide transformations during high-temperature oxidation of nickel-base superalloys. *Oxid. Met.* **2005**, *63*, 57–72. [CrossRef]

Disclaimer/Publisher's Note: The statements, opinions and data contained in all publications are solely those of the individual author(s) and contributor(s) and not of MDPI and/or the editor(s). MDPI and/or the editor(s) disclaim responsibility for any injury to people or property resulting from any ideas, methods, instructions or products referred to in the content.